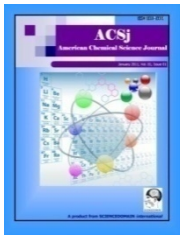

American Chemical Science Journal
4(4): 424-442, 2014

SCIENCEDOMAIN *international*
www.sciencedomain.org

Removal of Congo Red Dye Using an Adsorbent Prepared from *Martynia annua, L.* Seeds

V. Sivakumar[1*], M. Asaithambi[2], P. Sivakumar[3] and N. Gopal[2]

[1]Department of Chemistry, Sri Vasavi College, Erode, TN, India.
[2]Department of Chemistry, Erode Arts College, Erode, TN, India.
[3]Department of Chemistry, AA Govt Arts College, Namakkal, TN, India.

Authors' contributions

This work was carried out in collaboration between all authors. Author MA designed the study. Author VS performed the analysis, wrote the protocol and wrote the first draft of the manuscript. Authors VS and PS managed the analyses of the study. Authors VS and NG managed the literature search. All authors read and approved the final manuscript.

Original Research Article

Received 31st August 2013
Accepted 19th December 2013
Published 5th February 2014

ABSTRACT

Activated carbons M1 and M2 were prepared from the seeds of *Martynia annua, L.* using H_2SO_4 and H_3PO_4 as chemical activating agents respectively. In this study, utilization of these adsorbents for the removal of Congo red (CR) dye from aqueous solution was investigated. The physical, chemical and morphological properties were determined using XRD, BET and SEM techniques. Experiments of CR adsorption on the prepared adsorbents were conducted using batch technique and their results were also compared. The data were tested with five different isotherm models; it fitted to Langmuir isotherm for M1 and for M2, four of the isotherm models fit with high correlation coefficient. Maximum adsorption capacity (mg/g) obtained for M1 was 12.45 and 29.85 for M2. Pseudo-second-order kinetics explained the adsorption process much better with good correlation coefficient. The adsorption rate was film diffusion controlled during the initial stages, and in the later stages the rate was controlled by intra particle diffusion. Increasing the temperature of the system decreases the equilibrium time accompanied by exothermic removal of CR. These studies indicate that the prepared adsorbent showed good adsorption characteristics towards textile dyes.

**Corresponding author: Email: cvabavani@rediffmail.com;*

Keywords: Adsorbent; isotherm models; zero point charge; adsorption kinetics and agro waste.

1. INTRODUCTION

Textile fabrics are part of human life, and are mainly used to satisfy human needs. The modernized textile industry utilizes wide variety of specialty chemicals such as softeners, stain releasing agents, wetting agents and fixing agents. Different kinds of organic dyes are used in textile processing. This usage has resulted in discharging the coloured effluents containing dyestuffs [1]. The synthetic organic dyes are widely used for dyeing textile fiber such as cotton and polyester [2]. These substances are transported across the international boundaries far from their sources, and they persist in the environment and bioaccumulate through the food chain. This inflicts high risk to human health. The release of coloured wastewater into the ecosystem causes aesthetic pollution, eutrophication, and perturbation in aquatic life [3,4]. When this polluted water is used for irrigation, it gets evaporated and leaves salts caked on the surface of the farm lands. It finally spoils the texture of the soil [5]. Therefore, the removal of such coloured substances from effluents has great environmentaland commercial importance [6].

Direct or substantive dyes are a special class of dyes. Owing to their size and shape they readily penetrate cellulosic fibers. . Theyalso have a goodfiber affinity [7]. These dyes have a long narrow and a flat molecular structure, which allows them to readily enter into the cellulose structure and interact with the cellulose to provide good fiber affinity. The three methods of treatment generally employed for dye removal are: physical, chemical, and biological [8,9] methods. These include adsorption, nano filtration, ion exchange, coagulation-flocculation, precipitation, ozonisation, photodegradation, aerobic and anaerobic treatments [10]. Conventional physical and chemical methods are either costly or produces concentrated sludge and they are not capable of treating large volumes of effluent water without the risk of clogging [11]. The adsorption technology is often considered as an effective method for the treatment of dye effluents [12]. Easily available adsorbents like TiO_2, activated carbon, chitosan, montmorillonite, ash, bentonite, saw dust, silica and clay are used for this purpose. Most commonly used adsorbent for wastewater treatment is activated carbon [13]. Carbon adsorption is an expensive process and hence considerable interest for preparation of low cost adsorbents is palpable. This research is an attempt in this direction.

Recently many low cost adsorbents were derived from carbonaceous materials such as wood, coal and waste agricultural biomass. More availability of agricultural by-products makes them good sources of raw materials for the preparation of an activated carbon. Lots of studies have been carried out for the removal of different kinds of dyes using activated carbon derived from agricultural wastes. The most challenging task is the removal of anionic dyes, because they are bright coloured, water soluble, reactive and show acidic properties. Congo red (CR) is an example for anionic di-azo dye used in textile, printing, dying, paper and plastic industries [14]. It is also used in bio-chemistry and histology in microscopic preparations [15]. The treatment of contaminated wastewater containing CR is difficult, since the dye is generally present in the form of sodium salt making it highly soluble in water. The stability of its structure makes it difficult to biodegrade and photodegrade it [16]. Therefore it persists in the environment for a longer time [17].

In the past, attempts were made for the adsorptive removal of CR using chitoson [18], ethylenediamine modified rice hulls [19], hydrogen peroxide treated tendu waste [20], soil [21], bentonite [22], banana pith [23] and rice hull ash [24]. In this study, the adsorptive

removal of CR dye from aqueous solution using an activated carbon prepared from the seeds of *Martynia annua, L.* was investigated. As established in an earlier study [25], these agricultural wastes were subjected to various chemical treatments and then used for adsorption studies.

The influences of various operating parameters on adsorption, such as the effect of pH, influent dye concentration and temperature were studied. Equilibrium and kinetic parameters were studied to describe the velocity and mechanism of adsorption process and to determine the factors controlling the adsorption rate. The physical nature and surface morphology of the adsorbent were also analysed on the basis of their scanning electron micrograph (SEM) images, X- ray diffraction (XRD) and Brunauer–Emmett–Teller (BET) isotherm studies.

2. MATERIALS AND METHODS

2.1 Preparation of Adsorbent

Seeds of *Martynia annua, L.* collected from Erode District, Tamilnadu, India was used for the preparation of adsorbent. The seeds of the wild plant were thoroughly rinsed with water to remove the dust and soluble material and then it was dried at room temperature. The seeds were then treated with concentrated sulphuric acid. Charring of the hard seeds occurred immediately with evolution of fumes. After the reaction had subsided, the material was left in an air oven at 140-160ºC for a period of 24 hours. The dried mass was washed with excess of water to remove the free acid residues. It was dried at 110ºC and taken out to ground. The powdered material was then sieved and subjected for activation at 800ºC for a period of 10 minutes. This activated carbon was named as M1.

Seeds of *Martynia annua, L.* were soaked in 10% Phosphoric acid for a period of 24 hours. After impregnation, the mass was subjected to carbonization at 400ºC and was powdered into fine particles. It was washed with excess of water to remove the excess acid present and was then dried. The powdered material was then sieved and subjected for activation at 800ºC for a period of 10 minutes. This activated carbon was named as M2.

2.2 Characteristics of Adsorbent

The preparation and physico-chemical characterization of M1 and M2 activated carbons were already reported in the previous work [25]. Carbon particles sieved out of a mesh size of 300 to 180µ were used for the adsorption studies. The specific surface area and the pore structure of the carbon samples were determined by using a surface area and pore size analyzer (Micrometrics, ASAP 2020 V3.00 H Instrument) on nitrogen adsorption at -195.8ºC. The specific surface area was calculated using the BET equation. BET data of M1 and M2 were listed in Table 1. The microstructures of M1 and M2 carbons were observed by SEM (JOEL/EO 1.1 Model: JSM 5610) and are shown in Figs. 1a and 1b. The carbon samples were characterized by X- ray diffraction studies. To study these characteristics, Bruker X8 Single crystal KAPPA APEXII instrument with Copper anode radiation of Cu Kα (λ=1.5405 Å) was used at room temperature in the scanning angle (2θ) range of 5 to 89º. They were shown in Fig. 2.

Table 1. Textural characteristics of activated carbon

Carbon	S_{BET} (m^2/g)	Total pore Volume cm^3/g	Molecular cross-sectional area (nm^2)	Radius Range Å	Maximum Pore Volume (cm^3/g)	Median Pore Width Å	Qm cm^3/g STP
M1	0.967	0.9903: 0.0063	0.1620	-	-	-	0.2222
M2	401.10	0.9957: 0.1845	0.1620	8.500 to 1500.0	0.18451	6.343	92.14

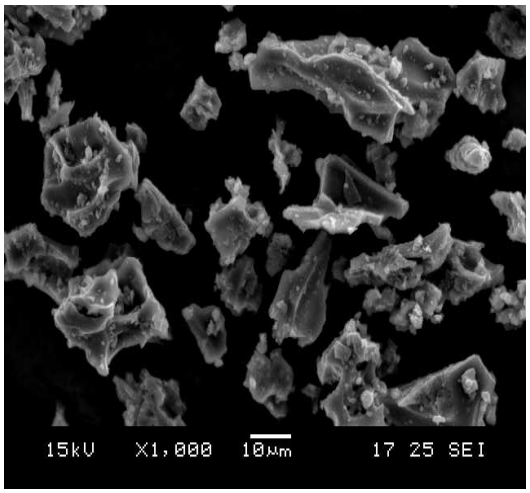

Fig. 1a

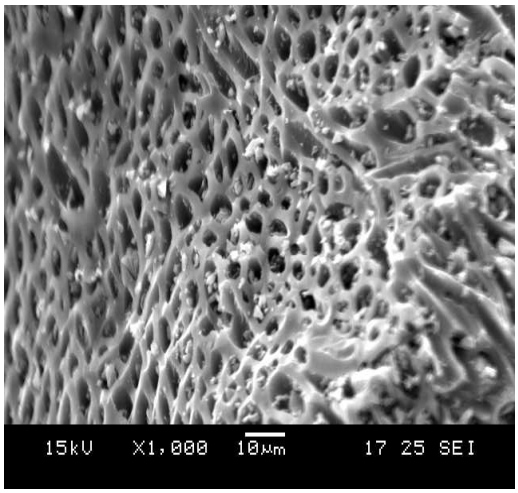

Fig. 1b

Figs. 1a and 1b - SEM images of M1 and M2

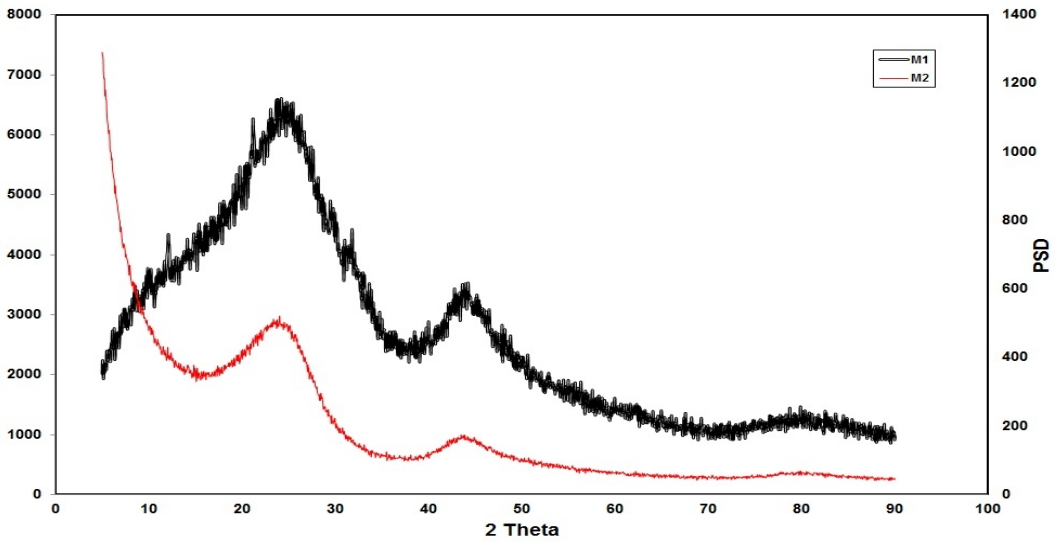

Fig. 2. XRD pattern for M1 and M2 at room temperature

2.3 Preparation of Adsorbate

The adsorbate, Congo red dye, was supplied by Chamundi Textiles (Silks Mills) LTD., Mysore, India. A stock solution of CR dye was prepared (1000 mg/L) by dissolving a required amount of dye powder (based on percentage purity) in deionised water. The stock solution was diluted with deionised water in order to obtain the desired concentration range of 10 to 75 mg/L. The concentration of CR in the experimental solution was determined by measuring the absorbance of solutions at λmax = 498 nm using an UV–Vis spectrophotometer (Perkin-Elmer).

2.4 Adsorption Studies

The pH of the solution was measured with an Elico pH meter (model LI 120), using a combined glass electrode. Adsorption experiments were carried out in 250-mL Erlenmeyer flasks. These flasks have a working volume of 100 mL dye solution and a fixed carbon dosage of 100 mg of the respective carbon. The initial pH of the solution was adjusted using 0.1 M NaOH or HCl as required. The flasks were shaken up to the specified time at 150 rpm in an orbital shaker (Rivotec).

The effect of initial pH for 50mg/L dye concentration was studied in the pH range from 2 to 12 with a fixed carbon dosage of 100mg. The solution was agitated for 2 hours at room temperature. The effect of temperature on adsorption for 75mg/L dye solution with a fixed carbon dosage (100mg/100mL) was studied at five different temperatures from 30 to 60ºC. The amount of dye adsorbed per unit mass of the adsorbent q_e mg/g and adsorption efficiency were calculated as follows:

$$q_e(mg/g) = (C_0 - C_e)\frac{V}{W} \quad (1)$$

$$\text{Efficiency (\%)} = \frac{(C_0 - C)}{C_0} \times 100 \quad (2)$$

Where C_0, C_e and C = initial, equilibrium and residual dye concentrations (mg/L) respectively.

3. RESULTS AND DISCUSSIONS

3.1 Adsorbent Characteristics

The scanning electron micrographs (SEM) of M1 and M2 were shown in Fig. 1a and 1b respectively. The SEM of M1 Fig. 1a indicates a heterogeneous, porous morphology. BET surface, specific surface area and micropore volume of the activated carbons M1 and M2 were measured by this method, employing Brunauer–Emmett–Teller (BET) correlation. The specific surface area of M2 was found to be larger (401.10 m²/g) when compared with M1 (0.967m²/g). Hence, it may be possible that the dye uptake by M1 was not governed by its surface area. The adsorption of the M1 may be due to the presence of various functional groups. Since carbon M2 had a reasonable amount of porosity, its adsorption is governed by the presence of long pores.

The results of XRD showed the presence of larger interlayer distances in the adsorbent that can help the dye molecule enter the interlayer gaps of the adsorbent. The broader peaks obtained for carbons can be attributed to the disordered structural alignment of carbon planes in activated carbons.

3.2 Effect of Solution pH Value on Dye Adsorption

The pH affects the structural stability of CR which leads to its colour intensity [22]. The experiments carried out at different pH levels ranging from 2 to 12 showed that there was a change in the per cent removal of CR over the entire pH range as shown in the Fig. 3. Aqueous solution of CR turned into blue colour at lower pH, and it turned red at higher pH. The interaction between dye and H^+ ions in the solution was higher at lower pH (pH=2). The maximum dye removal observed at this pH for M1 indicated that it contained more surface functional groups. The adsorption efficiency continuously decreased up to a pH of 6.0. Then the dye removal increased for both the carbons from pH 6.0 to pH 8.0. This increase in dye uptake may be because of the zero point charge density of the carbons. The reported pHzpc value of the carbon M1 was 7.5 and for M2 it was 7.1 [25]. As illustrated in Fig. 3, both the carbons showed an increased removal of CR on this pH range only. After a pH of 8.0, the adsorption decreased to 20% for M1 and 30% for M2. The surface of the adsorbents was negatively charged in the basic medium. Hence, it will not facilitate the attraction of negatively charged dye molecules in the basic medium (pH>8).

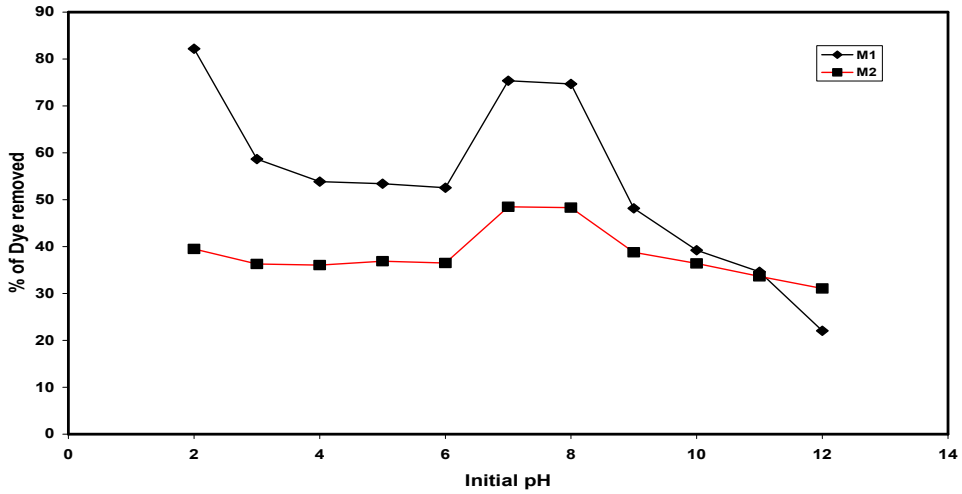

Fig. 3. Effect of pH for the adsorption of CR onto M1 and M2

Invariably, the activated carbon surfaces are associated with a certain amount of chemisorbed oxygen and hydrogen. These hetero atoms are derived from the raw material and become a part of the chemical structure. These hetero atoms form carbon-hydrogen, carbon-oxygen and other carbon-hetero atom surface complexes or surface groups. However, carbon-oxygen surface groups that are present on all activated carbons and pH of the solution are the two important parameters which determine the efficiency of the dye adsorption process. For each carbon, the pH value at which the surface charges corresponds to zero (nil charge) is known as zero point charge (and denoted as pHzpc). The carbon surface attains positive charge below its zero point charge and becomes negative above its zero point charge. In the aqueous phase, the dye is first dissolved and the

sulfonate groups of the dye (D-SO_3Na) are dissociated and converted to anionic dye ions at natural solution pH of 6.8 [22].

$$D - SO_3Na \rightarrow D - SO_3^- + Na^+$$

Since the carbon M1 was treated with a strong acid (H_2SO_4), it is acidic in nature. At lower pH, there is an excessive protonation which leads the carbon surface with more positive charges. To a considerable extent, this attracts the negatively charged dye (D-SO_3^-) from the solution phase by significant electrostatic attraction. As the pH of the system increased, the amount of H^+ ions decreased in the system. In order to maintain the electrical neutrality, the H^+ ions leave from –OH and –COOH groups from the surface of the solid phase. This led to the formation of O^- and COO^- sites on the carbon surface. This did not favor the dye adsorption in higher pH values. The carbon M2 was treatedwith phosphoric acid and relatively had lower H^+ ions in its surface compared with M1. It did not show higher adsorption in lower range of pH because of the absence of electrostatic interaction. On the other hand when the pH is equal to its pHzpc, the absence of surface charges on the adsorbent and dissociation of dye molecules helps the adsorption of CR significantly. The pH considerably affected the extent of dye removal on both the adsorbents and a reduction in the percentage of dye adsorption with increasing pH was observed in both cases. At lower pH values, strong electrostatic attraction was predominantly operating in M1. In M2, the maximum adsorption was observed only at pHzpc. As and when there was further increase in the pH, the surface of M2 got more negatively charged. Owing to the electrostatic repulsion, the adsorption of dye anions did not get increased.

3.3 Effect of Temperature and Agitation Time on CR Adsorption

The effect of temperature on the adsorption of CR (75mg/L) by M1 and M2 were carried out at five different temperatures from 30 to 60ºC Fig. 4. The rise in temperature increased the rate of diffusion of the adsorbed molecules across the external boundary layer and the internal pores of the adsorbent particles, owing to decrease in viscosity of the solution. It also changed the equilibrium capacity of the adsorbent for each specific adsorbate [26]. A decrease in sorptive removal of CR with increase in temperature for both the adsorbents was observed. It may partly be attributable to chemisorptions. Increase in temperature reduced the equilibrium time in both the carbons. In carbon M1, even a five degree rise in temperature (30 to 35ºC) decreased the dye removal by 7% and reduced the equilibrium time from 100 to 90 min. The amount of dye removal gradually decreased and it reached 37.8 mg/g at 60ºC. The adsorption rate was slightly decreased in the case of carbon M2 at equilibrium while increasing the temperature up to 40ºC. The equilibrium dye adsorption decreased in carbon M1 when rising the temperature up to 60ºC. In carbon M2 the amount of CR removal continuously decreased after 40ºC from 46 to 33 mg/g. With the increase in temperature there was an increase in the rate of the reaction was evidenced. The observed reduction in equilibrium time was attributable to decrease in the particle density, which from voids.

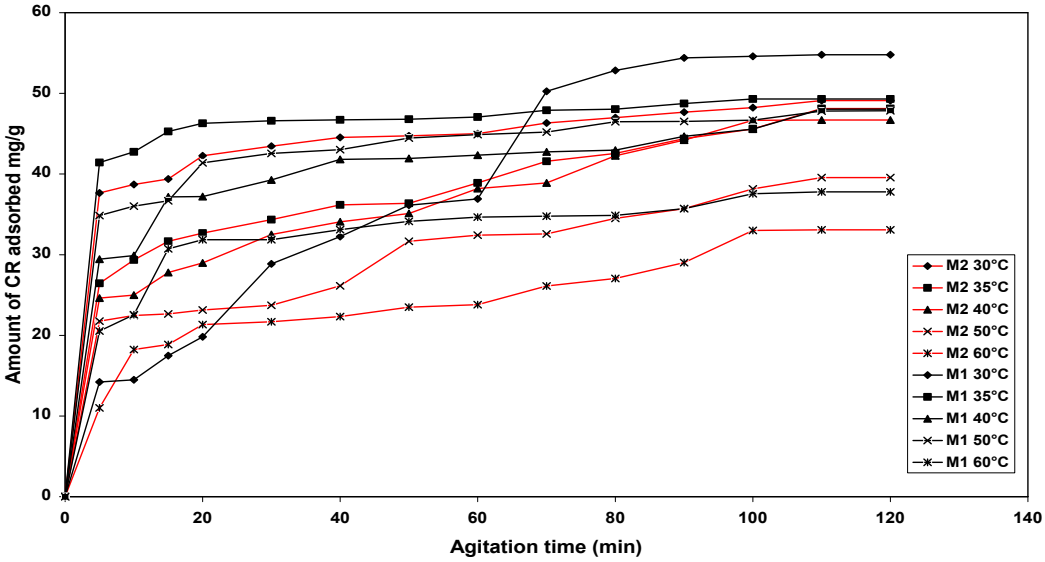

Fig. 4. Effect of temperature and agitation time for the adsorption of CR onto M1 and M2

Thermodynamic equilibrium parameters such as change in Gibbs free energy (ΔGº, J/mol), enthalpy (ΔHº, J/mol) and entropy (ΔSº, J/mol/K) were evaluated by:

$$\Delta G^{\circ} = -RT \ln K_C \tag{3}$$

Here, R is the universal gas constant (8.314 J/K/mol) and T is absolute temperature (K). The apparent equilibrium constant Kc (L/g) of the adsorption is defined as follows.

$$K_C = q_e / C_e$$

$$\ln K_C = \frac{\Delta S^{\circ}}{R} - \frac{\Delta H^{\circ}}{RT} \tag{4}$$

ΔHº and ΔSº were determined from the slope and intercept of linear plot of $\ln K_c$ versus 1/T. The negative values of ΔGº adsorbents (-2.7, -2.2, -1.7, -1.2 kJ/mol for M1 and -2.3, -1.9, -1.6,-1.2 kJ/mol for M2) indicated the spontaneous nature and feasibility of adsorption for CR onto the selected carbons. The negative value of ΔHº (-18.26 and -13.08 kJ/mol for M1 and M2 respectively) showed the exothermic nature of the adsorption, which is an indication of the existence of a strong interaction between the prepared adsorbent and CR. Again the negative enthalpy of adsorption indicated that the adsorption is spontaneous in nature. This suggested that the chemical bonds between the carbon surface and the dye molecules were strong enough and the dye molecules cannot be easily desorbed by physical means such as simple mechanical operation like shaking or thermal activity like heating. The negative value of ΔSº (-51.12, -35.54 J/K/mole for M1 and M2 respectively) showed the decreased randomness at the solid/solution interface during the adsorption of CR on M1 and M2,

reflecting the affinity of carbon for CR. During the adsorption there, some structural changes occurred and the system move in to more ordered state.

3.4 Adsorption Equilibrium- Isotherm Models

The mechanisms of adsorption were studied by various adsorption isotherms. Adsorption isotherm usually describes the equilibrium concentration of adsorbate in the bulk of the solution and amount adsorbed at the surface. Analysis of isotherm data is fundamentally important to predict the adsorption capacity of the adsorbent for designing an adsorption system. The data obtained in the present experiment were analysed using Langmuir, Freundlich, Temkin, Harkins–Jura and Halsey isotherm models. The linear and non-linear equations of these isotherm models were shown in Table. 2.

Table 2. Lists of adsorption isotherms models

Isotherm model	Nonlinear form equation	Linear form equation
Langmuir	$q_e = \frac{Q_0 b C_e}{1 + bC_e}$	$\frac{C_e}{q_e} = \frac{1}{Q_0 . b_L} + \frac{C_e}{Q_0}$
Freundlich	$q_e = K_f C_e^{1/n}$	$\log q_e = \log K_f + \frac{1}{n} \log C_e$
Temkin	$q_e = \left(\frac{RT}{b}\right) \ln(A.Ce)$	$q_e = \left(\frac{RT}{b}\right) \ln A + \left(\frac{RT}{b}\right) \ln C_e$
Harkins–Jura	$m = n \ln C_e + \frac{1}{q_e^2}$	$\frac{1}{q_e^2} = \left(\frac{B}{A}\right) - \left(\frac{1}{A}\right) \log C_e$
Halsey	$\ln q_e = \left[\left(\frac{1}{n}\right) \ln K\right] + \left(\frac{1}{n}\right) \ln \frac{1}{C_e}$	$\log q_e = (\frac{1}{n}) \log K + (\frac{1}{n}) \log \frac{1}{C_e}$

3.4.1 Langmuir model

A Plot of C_e/q_e against C_e for the adsorption of CR onto M1 and M2 was shown in Figs. 5a and 5b respectively. The Langmuir isotherm was found to be linear over the entire concentration range with good linear correlation coefficients ($(0.9868<R^2<0.9992$ for carbon M1 and $0.9311<R^2<0.9853$ for carbon M2).

Langmuir adsorption capacity (Q_0) decreased from 12.45 mg/g to 3.41 mg/g for M1 and 29.85 mg/g to 26.05 mg/g for M2. The adsorption energy (b_L) increased from 0.061 to 0.226 for M1 and it was from 0.027 to 0.069 for M2 with increase in temperature. It showed that higher the temperature, higher will be the swelling of the internal structure of the adsorbent materials to decrease the monolayer adsorption capacity values (Q_0) and accommodate more CR molecules on its surface. The monolayer adsorption capacity is comparable with the values reported for other low cost adsorbents [27-29].

The essential characteristics of Langmuir isotherm is expressed in terms of a dimensionless equilibrium parameter R_L.

$$R_L = \frac{1}{(1 + b_L C_0)} \quad (5)$$

Where C_0 is the initial concentration of CR in mg/L, R_L value indicates the type of adsorption isotherm to be either unfavorable (R_L>1), favorable (R_L<1), linear (R_L=1) or irreversible (R_L=0). The adsorption of CR on to M1 and M2 was favorable as evident from the calculated $R_L$values ($0.1650<R_L<0.3772$ for M1 and $0.3297<R_L<0.551$ for M2). The calculated values of Langmuir constant b_L, adsorption capacity Q_0, correlation coefficient R^2 and dimensionless equilibrium parameter R_L were given in Table 3.

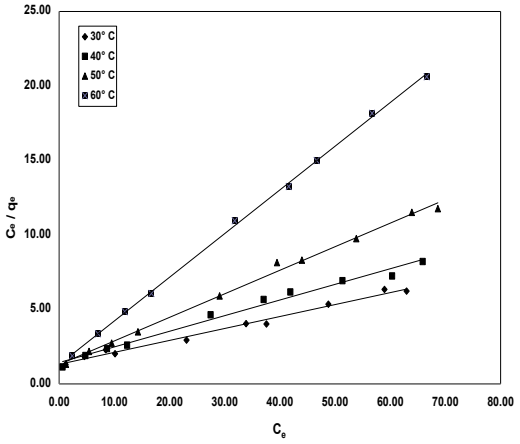

Fig. 5a

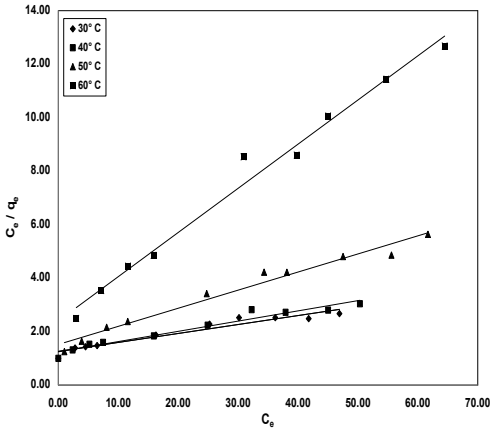

Fig. 5b

Figs. 5a and 5b- Langmuir plot for the adsorption of CR onto M1 and M2

3.4.2 Freundlich Model

This model can be applied to non-ideal and reversible multilayer adsorption systems on heterogeneous surfaces. The linearized form of Freundlich equation was given in Table 2. Where K_f is the measure of adsorption capacity (mg/g), n is the adsorption intensity, and are calculated from the intercept and slope of the linear plot of log q_e versus log C_e Figs. 6a and 6b and were listed in Table 3. The presence of chemisorption is confirmed if 1/n<1; and that of cooperative adsorption if 1/n>1 [30]. The calculated n values showed that at normal temperature, the dye adsorption was due to physical forces and when rising the temperature, chemical forces only predominate in both the carbons.

It was evident that the slope (1/n) decreased as the temperature increased and approached zero. This indicated that the surface became more heterogeneous and the possibility of swelling of the adsorption sites at the higher temperature. It was concluded that, at 30°C the CR removal includes cooperative adsorption and the surfaces were homogeneous in nature. At higher temperature, the surfaces became more heterogeneous and chemisorption process prevailed. Both the carbon samples indicated that the adsorption of CR was favorable. The experimental data fitted well for this equation with high correlation coefficient values for M1 ($0.88<R^2<0.896$) and M2 ($0.9512<R^2<0.9876$).

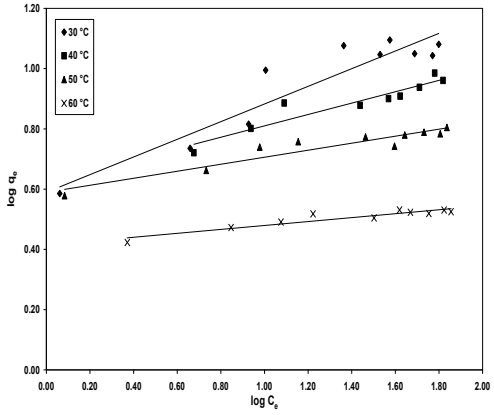

Fig. 6a

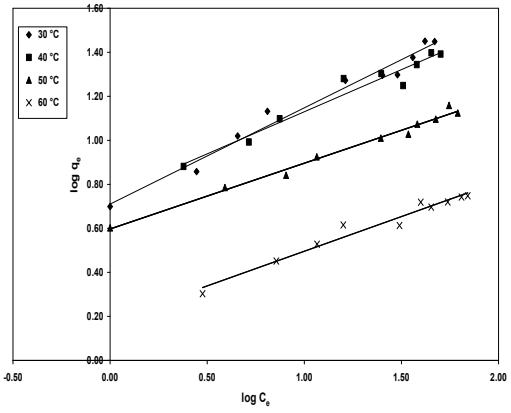

Fig. 6b

Figs. 6a and 6b – Freundlich plot for the adsorption of CR onto M1 and M2

3.4.3 Temkin model

The linear and nonlinear forms of Temkin equation were given in Table 2. Where A is the equilibrium binding constant corresponding to the maximum binding energy (L/mg), B is Temkin isotherm constant (J/mol) related to heat of adsorption (function of temperature) and R is the gas constant (8.314J/K/mole). The values of the Temkin constants A and B were calculated from the intercept and slope respectively, and correlation coefficients were listed in Table 3, from the linear plot of lnC_e versus q_e Fig. not shown. This model contains a factor based on adsorbate- adsorbent interactions [31].

The maximum binding energy (A) was noted in M1 (41524 L/mg) at 60ºC implied that the interaction of CR molecules with the adsorption sites was more at higher temperature. The value of heat of adsorption B was high at 30ºC and it was further decreased when increasing the temperature. This indicated that at the lower temperature, more CR molecules got adsorbed on M1; hence the heat of adsorption was more (2.202 J/mol). In M2, the value of A increased to larger extent (1.52 to 3.36 L/mg) when the temperature changed from 30ºC to 50ºC. This implies that the system was influenced by thermal properties as shown in the maximum binding energy (A). Whereas at lower temperature, the heat of adsorption (B) was more (5.99 J/mole at 30ºC) and it decreased drastically at higher temperature (1.15 J/mole at 60ºC).

Temkin isotherm represented a fair fit with experimental data. The obtained R^2 values for M1 and M2 were ($0.8588<R^2<0.9021$) and ($0.9298<R^2<0.9643$) respectively. This suggested that CR removal on M1 was limited with monolayer coverage. The surface of M1 was relatively homogeneous in terms of functional groups.

There must be a noteworthy interaction with dye molecules by the adsorbents that fit the data with high R^2 values for Langmuir equation than Freundlich and Temkin equations. The Freundlich and Temkin isotherms are used for heterogeneous surface energy systems, the carbon M2 had more active sites, and they were filled with dye molecules until the lowest energy sites were filled at the end of the adsorption process.

3.4.4 Harkins–Jura model [32]

The linear and nonlinear form of Harkins-Jura isotherm equations were given in Table 2. Where C_e is the equilibrium concentration of CR in solution (mg/L), q_e is the amount of CR adsorbed onto the adsorbent (mg/g) and A and B are isotherm constants. The Harkins-Jura adsorption isotherm accounts to multilayer adsorption and can be explained with the existence of a heterogeneous pore distribution. $1/q_e^2$ was plotted vs. log C_e Fig. not shown and the isotherm constants, correlation coefficient values were listed in Table 3. This method can be employed when different types of pores are involved in an adsorbent. Both the carbon samples had slits and spherical pores on its surface. It was confirmed by its SEM images and data obtained from XRD studies. The obtained data were fairly fitted with equation and yields R^2 values for M1 ($0.8363<R^2<0.8618$) and M2 ($0.7905<R^2<0.8573$). The constant A for the adsorption of CR onto M1 increases while increasing the temperature from 30ºC to 40ºC and the constant B decreases while increasing the temperatures, which accounts the heterogeneous nature of M1. When the adsorption proceeds, the accumulation of dye particles on the surfaces at higher temperatures was not favored. The correlation coefficients obtained for both carbons were not high; this indicated least existence of the multi-layered adsorption.

3.4.5 Halsey model [33]

The Halsey isotherm model is used for heteroporous solids. It is suitable for multilayer adsorption. The equation was given in Table 2. Where K is the Halsey isotherm constant and n is the exponent. Plot of $1/C_e$ vs. ln q_e gave a positive slope Fig. not shown which is equal to 1/n and the value of K was calculated from the intercept. The calculated results were listed in Table 3.

The existence of long pores favored the multi-layer adsorption in M2 and the data obtained were fitted with high correlation coefficient values ($0.9512<R^2<0.9876$). This implied the presence of physical forces in the adsorption process at the lower temperature. The existence of Vander walls forces was ruled out in the adsorption of CR on to M1 because the obtained data were poorly fitted with the equation ($0.88<R^2<0.896$). The existence of surface heterogeneity was ruled out in the adsorption of CR on to M1 because of poor correlation coefficient and therefore, the adsorption was chemisorption in nature.

3.5 Adsorption Kinetics

Adsorption kinetics show large dependence on the physical and chemical characteristics of the adsorbent material, and presence of adsorbate in bulk. In the present work, in order to examine the controlling mechanism of sorption processes such as mass transfer and chemical reaction, pseudo first-order, pseudo second-order, intraparticle diffusion and Elovich kinetic models were used.

3.5.1 Pseudo-first order kinetic model

The linear form of first- order kinetic equation is

$$\log(q_e - q_t) = \log q_e - \left(\frac{k_1}{2.303}\right)t \quad (6)$$

Where q_e and q_t are the amounts of CR adsorbed at equilibrium and at time t (min) respectively; k_1 is the first-order rate constant (min^{-1}). Linear plot of log (q_e-q_t) versus t was made and values of k_1 and q_e were obtained from the slope and intercept Fig. not shown and were given in Table 4.

The result showed that the adsorption of CR onto M1 did not follow the first order kinetics. At the given temperature, the first-order rate constant (k_1) increased with the increase in initial dye concentration. At higher initial dye concentration, the number of available binding sites at the M1 surface, per adsorbate molecule increased. The obtained R^2 and q_e values for carbon M2 showed the dye removal process did not follow first order kinetics. The adsorption data fitted poorly with pseudo-first order kinetic model for both carbon samples and the calculated q_e values did not agree with the experimental q_e values at all concentrations. Hence the adsorption did not follow first order rate expression for both the carbons. The CR removal process did not depend on either the concentration of adsorbent system or adsorbate availability in the bulk.

3.5.2 Pseudo-second order kinetic model

Pseudo second-order model rate equation is represented as

$$\frac{t}{q_t} = \frac{1}{k_2 q_e^{\,2}} + \frac{1}{q_e} t \quad \text{where } h = k_2 q_e^{\,2} \tag{7}$$

h represents the initial adsorption rate (mg/g/min) and k_2 is the second order rate constant (g/mg/min). The values of k_2 and q_e were calculated from the intercept and slope of the t/q_t versus t plots as shown in Fig 7a and 7b. The results obtained were given in Table 4. It was observed from Table 4 that there was a good agreement between experimental and calculated q_e values with high correlation coefficient values for both the carbons. Hence the pseudo second-order model better represented the adsorption kinetics between the carbon and CR. The adsorption process depended on the concentration of both adsorbent and adsorbate. The rate of adsorption depended on the concentration of carbon and CR molecules in the bulk.

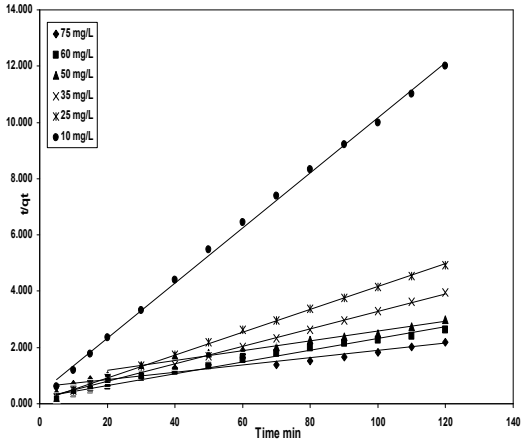

Fig. 7a

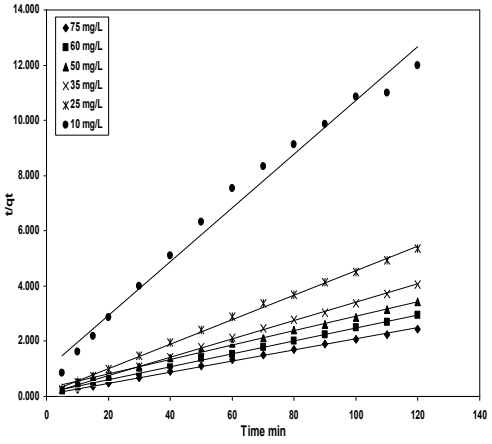

Fig. 7b

Figs. 7a and 7b- Pseudo-second order plot for the adsorption of CR onto M1 and M2

3.5.3 Weber- morris model

The Weber-Morris or Intraparticle diffusion model describes the adsorption of dye solutes from solution by porous carbon by three consecutive steps [34]. The first step is the transport of the dye from the bulk solution to the outer surface of the carbon by molecular diffusion. This is called external or film diffusion. The concentration gradient in the liquid film around the carbon surface is the driving force in film diffusion. The second step, called internal diffusion, which involves the transport of the dye from the carbon surface into interior sites by diffusion within the pore filled liquid and migration along the solid surface of the pore. These two steps act in parallel, the rapid one will control the overall rate of transport. The third and final step is adsorption of the dye on the active sites on the interior surface of the pores. The overall rate of the adsorption process will be controlled by the slowest step among the three steps. Since adsorption step is very rapid one, the rate controlling step is either film diffusion or internal diffusion. The nature of the rate determining step in batch systems can be determined from the properties of solute and adsorbent. Rates of adsorption are usually measured by determining the change in concentration of the dye in contact with the carbon as a function of time.

The intraparticle diffusion equation is given as

$$q_t = K_p t^{\frac{1}{2}} + C \tag{8}$$

Where K_p is the intra-particle diffusion rate constant (mg/g $min^{½}$) and C is intercept. A plot between amount of dye adsorbed per unit mass of adsorbent q_t and $t_{1/2}$ was shown in Figs. 8a and 8b. The obtained R^2 and K_p values were shown in Table 4. From the plots, it was concluded that the adsorption of CR by M1 was film diffusion controlled at concentrations less than 35mg/L and a direct linear relationship existed between the initial CR concentration and adsorption rate. If the concentration of CR exceeded 35 mg/L, the adsorption was intraparticle diffusion controlled. In carbon M2, if the CR concentration exceeded 25 mg/L, the process was controlled by intraparticle diffusion.

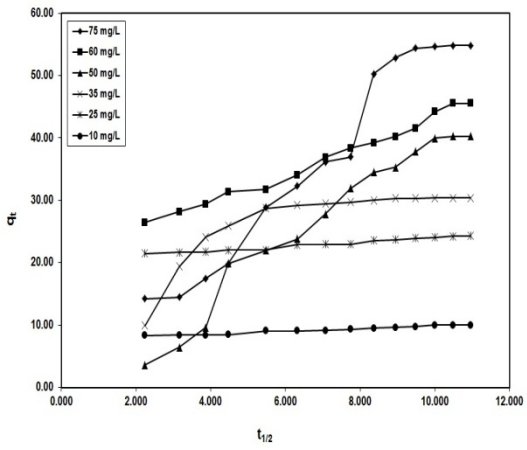

Fig. 8a

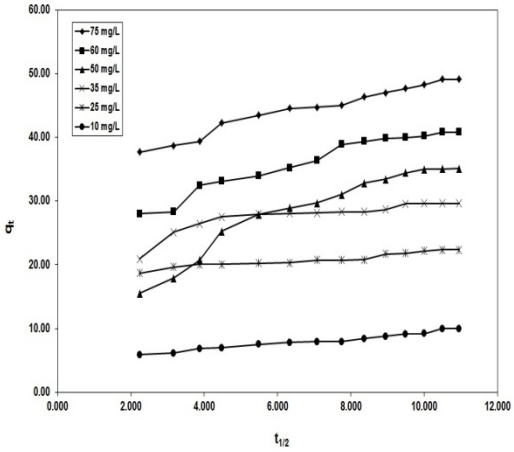

Fig. 8b

Figs. 8a and 8b- Intraparticle diffusion plot for the adsorption of CR onto M1 and M2

Table 3. Results of various Isotherm models

Models	Parameters	30ºC		40ºC		50ºC		60°C	
		M1	M2	M1	M2	M1	M2	M1	M2
Langmuir	Q_0 mg/g	12.45	29.85	9.52	26.109	6.321	14.837	3.411	6.053
	b L/mg	0.0611	0.0266	0.0735	0.0308	0.1215	0.4437	0.2265	0.0688
	R_L	0.3772	0.551	0.3415	0.5198	0.2530	0.4091	0.1650	0.3297
	R^2	0.9868	0.9311	0.9864	0.951	0.9959	0.9738	0.9992	0.9853
Freundlich	K_f mg/g	3.88	5.13	4.18	5.59	3.89	3.95	2.59	1.51
	n	3.41	2.29	5.29	2.61	8.60	3.34	15.29	3.17
	1/n	0.293	0.437	0.189	0.383	0.116	0.299	0.065	0.315
	R^2	0.8811	0.976	0.885	0.9512	0.896	0.9876	0.88	0.9641
Temkin	A L/mg	4.43	1.52	12.11	1.35	716.3	3.36	41524	1.77
	B J/mole	2.20	5.99	1.36	5.65	0.58	2.43	0.19	1.15
	R^2	0.8588	0.932	0.8646	0.9298	0.9021	0.9363	0.8854	0.9643
Halsey	n	-3.4	-2.3	-5.3	-2.6	-11.7	-3.3	-15.3	-3.2
	K	$9.7x10^{-3}$	$1.8x10^{-4}$	$5.2x10^{-4}$	$1.1x10^{-2}$	$8.6x10^{-6}$	$1x10^{-2}$	$4.7x10^{-7}$	$2.6x10^{-1}$
	R^2	0.8811	0.976	0.8885	0.9512	0.896	0.9876	0.88	0.9641
Harkins-Jura	A	31.5	52.3	55.9	94.3	43.1	33.8	30.2	7.4
	B	1.8	1.5	2.4	1.7	2.8	1.7	4.4	1.9
	R^2	0.8363	0.7905	0.8448	0.8735	0.8549	0.8973	0.8618	0.8452

As seen from Table 3, the Langmuir isotherm provided the best correlation for the experimental data for both prepared adsorbents, whereas Freundlich, Temkin and Halsey isotherm models well agreed the experimental data for M2 with high correlation coefficient values

Table 4. Results of kinetics plots for the adsorption of CR onto carbon M1 and M2

Initial CR concentration mg/L	$q_{e,exp}$ mg/g	Pseudo-first-order kinetic model			Pseudo-second-order kinetic model			Elovich model			Intraparticle Diffusion model	
		$q_{e,cal}$mg/g	k_1 min	R^2	$q_{e,cal}$mg/g	k_2x10^{-2} g/mg/min	R^2	αmg/g/min	β g/mg	R^2	K_p	R^2
(M1)												
75	54.79	95.5	0.0507	0.8483	83.33	236.0	0.9224	4.08	0.063	0.9043	3.74	0.9602
60	45.55	27.8	0.0230	0.8921	50.0	17.0	0.9875	49.48	0.157	0.9209	2.40	0.9782
50	39.54	73.6	0.0461	0.7977	71.43	17.3	0.9035	2.49	0.078	0.9728	2.13	0.9999
35	30.37	22.2	0.0670	0.968	32.26	52.5	0.9977	19.53	0.185	0.8228	0.41	0.9948
25	24.3	6.87	0.0363	0.8158	25.0	1.7	0.9993	$2.7x10^{-8}$	1.008	0.9000	0.43	0.8901
10	10.0	3.01	0.0272	0.7870	10.20	2.7	0.9984	$6.0x10^{-4}$	1.650	0.9025	0.14	0.833
(M2)												
75	49.10	17.5	0.0286	0.8729	50.0	48.1	0.9985	$1.06x10^{4}$	0.2613	0.9691	0.85	0.9318
60	40.78	20.2	0.0366	0.9503	42.37	42.0	0.9984	$3.48x10^{2}$	0.2225	0.9663	1.19	0.9865
50	35.09	30.6	0.0483	0.9475	38.31	68.3	0.9976	$1.23x10^{2}$	0.1502	0.984	1.32	0.9794
35	29.62	9.51	0.0403	0.7430	30.12	1.28	0.9994	$1.46x10^{4}$	0.4513	0.8629	0.30	0.9801
25	22.37	1.36	0.0286	0.7535	22.62	1.47	0.9982	7.7×10^{6}	0.9357	0.8881	0.21	0.8725
10	10.0	5.24	0.0188	0.8882	10.27	96.3	0.9856	17.92	0.7903	0.9165	0.19	0.8489

It is very much recognized that the adsorption rate is film diffusion controlled during the initial stages and the reaction rate is controlled by intraparticle diffusion when the carbon loaded with dye molecules.

3.5.4 Elovich model

The adsorption data is analysed by using the Elovich equation which has the form

$$\frac{dq_t}{dt} = \alpha \exp^{-\beta q_t} \tag{9}$$

Where α is the initial adsorption rate constant (mg/g/min) and β is related to the extent of surface coverage and activation energy for chemisorption (g /mg). If we assume αβ>>1 and the integration of the rate equation with the same boundary conditions as the pseudo first-order and second-order equations becomes the Elovich equation

$$q_t = \left(\frac{1}{\beta}\right)\ln \alpha\beta + \left(\frac{1}{\beta}\ln t\right) \tag{10}$$

The values of α, β calculated from intercept and slope of the plot lnt vs. q_t Fig. not shown and the results were listed in Table 4 along with R^2 values.

α and β parameters derived from Elovich equation to estimate reaction rates. It was suggested that an increase in α value and/or decrease in β value would increase the rate of the adsorption process. The obtained R^2 values for both the carbons for all the concentrations were high ($0.8228<R^2<0.9728$ for M1 and $0.8629<R^2<0.984$ for M2). This suggested that Elovich model best described this adsorption system.

4. CONCLUSION

Activated carbons (M1 and M2) were prepared from the seeds of *Martynia annua, L.* using Sulphuric acid and Phosphoric acid as the respective activating agents. The efficacy of adsorption studied revealed the following results.The specific surface area of M2 was found to be more (401.10 m²/g) compared with M1 (0.967m²/g). The prepared adsorbents were tested for their adsorption ability towards a textile dye. The direct dye Congo red had considerable affinity for M1 and M2. Lower pH was very effective for the removal of CR on M1. Adsorption decreased with increasing the pH. Both the carbons showed an enhanced dye removal only at their respective pHzpc. Effect of temperature on adsorption minimized the time required to attain equilibrium. The obtained thermodynamic parameters indicated that the adsorption was spontaneous and exothermic in nature (ΔHº = -18.26 and -13.08 kJ/mol). The study also proved that the decreased randomness (ΔS° = -51.12 and -35.54 J/K/mole) at the solid/solution interface. Out of five isotherm models used, the Langmuir, Freundlich and Temkin models fitted the data with high correlation coefficients. The kinetics of CR adsorption onto M1 and M2 followed the pseudo-second order kinetics. The initial stage of adsorption followed film diffusion mechanism and the later stages were controlled by intraparticle diffusion. Activated carbons prepared from *Martynia annua, L.* seeds were, therefore a promising adsorbent for the removal of dyes from the effluents of textile processing industries.

COMPETING INTERESTS

Authors have declared that no competing interests exist.

REFERENCES

1. Chiou MS, Ho PY, Li HY. Adsorption of anionic dyes in acid solutions using chemically cross-linked chitosan beads. Dyes Pigments. 2004;60:69–84.
2. Tsai WT, Chang CY, Ing CH, Chang CF. Adsorption of acid dyes from aqueous solution on activated bleaching earth. J Colloid Interf Sci. 2004;275:72-78.
3. Sauer T, CesconetoNeto G, Jos´e HJ, Moreira RFPM. Kinetics of photocatalytic degradation of reactive dyes in a TiO_2 slurry reactor. J Photochem Photobiol A. 2002;149:147–154.
4. Vandevivere PC, Bianchi R, Verstraete W. Treatment and reuse of waste water from the textile wet-spinning industry: review of emerging technologies. J Chem Technol Biotechnol. 1998;72:289-302.
5. Sivakumar V, Asaithambi M, Jayakumar N, Sivakumar P. Assessment of the Contamination from the Tanneries & Dyeing Industries on to Kalingarayan Canal of Tamil Nadu. Int J Chem Tech Res. 2010;2:774-779.
6. Ozacar M, SengilIA. Equilibrium data and process design for adsorption of disperse dyes on to alunite. Environ Geol. 2004;45:762-768.
7. Bulut Y, Aydin HA. Kinetics and thermodynamics study of methylene blue adsorption on wheat shells. Desalination. 2006;194:259-267.
8. Slokar YM, Majcen Le Marechal A. Methods of decolouration of textile wastewater. Dyes Pigments. 1998;37:335-336.
9. Hao OJ, Kim H, Chiang PC. Decolorization of wastewater, Crit. Rev Environ Sci Technol. 2009;30:449-505.
10. Bellir K, Sadok Bouziane I, Boutamine Z, Bencheikh Lehocine M, Meniai AH. Sorption study of a basic dye “Gentian Violet” from aqueous solutions using activated bentonite. Energy Procedia. 2012;18:924-933.
11. Robinson T, McMullan G, Marchant R, Nigam P. Remediation of dyes in textile effluent: a critical review on current treatment technologies with a proposed alternative. Bioresource Technol. 2001;77:247-255.
12. Reife A, Freeman HS. Environmental chemistry of dyes and pigments, New York: Wiley; 1996.
13. Malavizhi R, Ming-Huang Wang, Yuh-Shan HO. Research trends in adsorption technologies for dye containing waste waters. World appl Sci J. 2010;8:930-942.
14. Purkait MK, Maiti A, DasGupta S, De S. Removal of Congo red using activated carbon and its regeneration. J Hazard Mater. 2007;145:287-295.
15. Vijayakumar G, Dharmendirakumar M, Renganathan S, Sivanesan S, Baskar G, Kuppannagounder PE. Removal of Congo red from aqueous solutions by perlite. Clean-Soil Air Water. 2009;37:355-364.
16. Vimonses V, Lei S, Jin B, Chow CWK, Saint C. Adsorption of Congo red by three Australian kaolins. Appl Clay Sci. 2009;43:465-472.
17. Gharbani P, Tabatabaii SM, Mehrizad A. Removal of Congo red from textile waste water by ozonation. Int J Environ Sci Tech. 2008;5:495-500.
18. Chatterjee Sudipta, Dae SLee, Min WLee, Seung HWoo. Enhanced adsorption of Congo red from aqueous solutions by chitosan hydrogel beads impregnated with cetyltrimethyl ammonium bromide. Bioresource Technol. 2009;100:2803-2809.

19. Siew-Tengong, Eng Hooi Tay, Sie-Tiong Ha, Weng-Nam Lee, Pei-Sin Keng. Equilibrium and continuous flow studies on the sorption of Congo red using ethylenediamine modified rice hulls. Int J Phy Sci. 2009;4-11:638-690.
20. Nagda GK, Ghole VS. Biosorption of Congo red by Hydrogen Peroxide treated Tendu Waste. Iran. J Environ Health Sci Eng. 2009;6:195-200.
21. Smaranda C, Gavrilescu M, Bulgariu D. Studies on sorption of Congo red from aqueous solution on to soil. Int J Environ Res. 2011;5:177-188.
22. Emrah Bulut, Mahmut Ozacar, Ayhan Sengil I. Equilibrium and kinetic data and process design for adsorption of Congo red on to bentonite. J Hazard Mater. 2008;154:613-622.
23. Namasivayam C, Kanchana N. Removal of Congo red from aqueous solution by waste banana pith. Pertanika J Sci & Technol. 1993;1:33-42.
24. Kan-Sen Chou, Jyh-Ching Tsai, Chieh-Tsung Lo. The sorption of Congo red and vacuum pump oil by rice hull ash. Bioresource Technol. 2001;78:217-219.
25. Vadivel Sivakumar, Manickam Asaithambi, Ponnusamy Sivakumar. Physico-chemical and adsorption studies of activated carbon from Agricultural wastes. Adv App Sci Res. 2012;3:219-226.
26. Al-Qodah Z. Adsorption of dyes using shale oil ash. Water Res. 2000;34:4295-4303.
27. Rao VVB, Rao SRM. Adsorption studies on treatment of textile dyeing industrial effluent by fly ash. Chem Eng J. 2006;116:77-84.
28. Mall ID, Srivatsava VC, Agarwll NK, Mishra IM. Removal of Congo red from aqueous solution by bagasse fly ash and activated carbon: kinetic study and equilibrium isotherm analysis. Chemosphere. 2005;61:492-501.
29. Tor A, Cengeloglu Y. Removal of Congo red from aqueous solution by adsorption on to acid activated red mud. J Hazard Mater. 2006;138:409-415.
30. Haghseresht F, Lu G. Adsorption characteristics of phenolic compounds onto coal-reject derived adsorbents. Energy Fuels. 1998;12:1100-1107.
31. Foo KY, Hameed BH. Insights into the modeling of adsorption isotherm systems. Chem Eng J. 2010;156:2-10.
32. Harkins WD, Jura EJ. The decrease of free surface energy as a basis for the development of equations for adsorption isotherms; and The Existence of Two Condensed Phases in Films on Solids. J Chem Phys. 1944;12:112-113.
33. Basar CA. Applicability of the various adsorption models of three dyes adsorption onto activated carbon prepared waste apricot. J Hazard Mater. 2006;135:232–241.
34. Karadag D, Koc Y, Turan M, Armagan B. Removal of ammonium ion from aqueous solution using natural Turkish clinoptilolite. J Hazard Mater. 2006;136:604-609.

Peer-review history:
The peer review history for this paper can be accessed here:
http://www.sciencedomain.org/review-history.php?iid=424&id=16&aid=3541